



Article

Tribological Characterization of Carbon Nanotube/Aluminum Functionally Graded Materials Fabricated by Centrifugal Slurry Methods

Hideaki Tsukamoto

Department of Mechanical Engineering, Graduate School of Science and Engineering, Hosei University, 3-7-2 Kajino-cho, Koganei-shi, Tokyo 184-8584, Japan; htsukamoto@hosei.ac.jp

Abstract: Although carbon nanotube (CNT) is a promising material due to its excellent mechanical and functional properties, CNT has not been effectively used for high performance composites due to the degradation of its mechanical properties as a result of insufficient dispersibility of CNT in its matrix. In this study, CNT/aluminum (Al) matrix functionally graded materials (FGMs) were fabricated by centrifugal slurry methods. The dispersion of CNT was carried out with the solvent of dimethylacetamide (DMAs), and the dispersant of potassium carbonate (K_2CO_3) under ultrasonic sonication conditions. Tribological characteristics on the FGMs were investigated using a ball-on-disk tribometer. It was demonstrated that the presence of CNT contributed to an increase of the coefficients of friction and an enhancement of wear resistances.

Keywords: carbon nanotube; aluminum; functionally graded materials (FGMs); centrifugal slurry method; frictional characteristics



Citation: Tsukamoto, H. Tribological Characterization of Carbon Nanotube/Aluminum Functionally Graded Materials Fabricated by Centrifugal Slurry Methods. *J. Compos. Sci.* **2021**, *5*, 254. <https://doi.org/10.3390/jcs5100254>

Academic Editor: Oscar Marcelo Suárez

Received: 9 September 2021
Accepted: 20 September 2021
Published: 24 September 2021

Publisher's Note: MDPI stays neutral with regard to jurisdictional claims in published maps and institutional affiliations.



Copyright: © 2021 by the author. Licensee MDPI, Basel, Switzerland. This article is an open access article distributed under the terms and conditions of the Creative Commons Attribution (CC BY) license (<https://creativecommons.org/licenses/by/4.0/>).

1. Introduction

Much attention has been paid to application of carbon nanotube (CNT) in both scientific and industrial fields in the past decades due to its excellent physical and chemical properties such as its high strength, high elastic modulus, high thermal conductivity, and low density. CNT is a tube-like shape of carbon with a diameter on the nanometer scale. From the number of carbon layers, CNT can be classified into two types of CNT, that is single-walled carbon nanotubes (SWCNT) and multi-walled carbon nanotubes (MWCNT). Due to its excellent properties, CNT can play a significant role in the fields of nanotechnology, electronics, optics and others. CNT can be expected as an *irreplaceable* reinforcement of metal matrix composites (MMCs) [1–12].

Attempts to develop CNT/aluminum (Al) matrix composites with enhanced strength have been highly attractive, and can produce suitable structural materials in the aerospace and automobile industries. However, at present, there are very few practical examples due to the difficulty in obtaining uniform dispersion and wetting of CNT with the matrix. Most bulk CNT/Al composites exhibit poorer mechanical properties than expected. Great efforts have been made to prepare such CNT/metal composites with homogeneous distribution as well as high volume fraction of CNT simultaneously. It can be accompanied with difficulty to represent uniform dispersion of the reinforcements into the matrix without damaging the nanotubes [13–17]. It was proposed that in order to tackle such problems, that is, take advantage of high performance of CNT in the composites, CNT was dispersed in a solvent of dimethylacetamide (DMAc) with a dispersing agent of potassium carbonate (K_2CO_3), which is an inorganic salt, under ultrasonic conditions [18].

Functionally graded materials (FGMs) are practically innovative concepts to protect the materials and structures working under super high temperatures and temperature gradients. FGMs are multi-phase composites which can be engineered with gradual spatial variations of constituents, resulting in smooth variation of thermal, mechanical and electrical properties. Strong points of FGMs to two dissimilar materials joined directly include

smoothing of thermal stress distributions across the layers, minimization or elimination of stress concentrations and singularities at the interface corners and an increase in bonding strength [19–23]. These advantages are achieved by making the FGMs with a predetermined gradual spatial variation of the volume fractions and microstructure of the material constituents according to functional performance requirements.

There have been many fabrication techniques for FGMs such as chemical and physical vapor depositions, plasma spray methods, centrifugal casting or centrifugal slurry, and a variety of powder metallurgical techniques. FGMs can have two manners of gradual transition of properties from one side to the other. One is a continuous gradient manner and another is a stepwise manner [24]. Centrifugal techniques lead to formation of a continuous gradient manner in FGMs. Centrifugal casting can be performed by addition of hard particles to a molten metal, which are mixed and poured into a rotating mold. The materials are solidified in the mold under centrifugal force producing a gradient of the hard particles in the metals, which depends on the size of particles, mold rotational speed, density and viscosity of the molten metal as well as the rate of solidification [25–28]. Centrifugal techniques were also applied with slurry consisting of mixture of ingredient powders and some liquids [26]. However, it has been mostly reported that centrifugal techniques for fabrication of FGMs are employed for only particle type of reinforcements, not fibers or fillers like CNT.

In this study, CNT/Al matrix FGMs were fabricated using centrifugal slurry methods. Some chemical treatments were applied to processes of making CNT apart each other in solvent of DMAc with dispersant of K_2CO_3 under ultrasonic sonication conditions. Tribological characteristics such as frictional force and wear resistance for CNT/Al matrix FGMs were investigated using a ball-on-disk tribometer.

2. Experimental Procedure

2.1. Fabrication

MWCNT with a diameter of 6–10 nm and with a length of 2–10 μm was used (supplied by CNano Technology Co., Ltd., Jiangsu, China through Marubeni Information Systems (MSYS) Co., Ltd., Tokyo, Japan). Al powders with a diameter of less than 30 μm (supplied by Kojundo Chemical Laboratory Co., Ltd., Saitama, Japan) were also used. CNT is cohesive and cannot exhibit inherit excellent properties unless dispersing CNT to the level of each one in the matrix. CNT was dispersed with the solvent of DMAc, and the dispersing agent of K_2CO_3 . The concentration of CNT to organic solvent was 1.0 mg/mL, and the concentration of dispersant to organic solvent was 0.2 mg/mL. Figure 1 shows the schematic illustration of CNT dispersing processes. Ultrasonic treatment was employed for dispersing CNT. The treatment was conducted for 2 h. The slurry of CNT was filtered using filter paper, and the CNT was taken out. A mixed powder was prepared from CNT and Al powders. The mixing ratios (volume fractions) of CNT and Al powders were 0.3% and 99.7%, respectively.

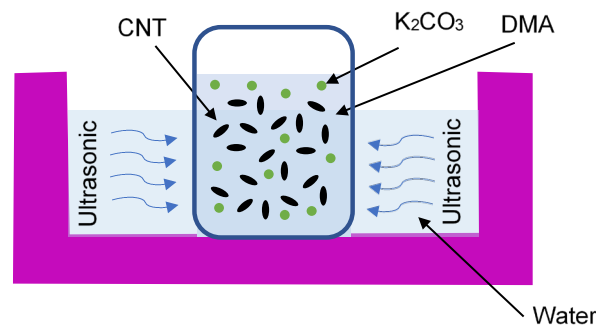


Figure 1. Schematic illustration of dispersion processes for CNT.

Centrifugal slurry methods were carried out. The mixed powder slurry was set in the mold in the centrifugal slurry equipment, as shown in Figure 2. Centrifugal operation was conducted with the rotation speeds of 150~450 rpm in steps of 50 rpm for 120 s. After the operation, the mixtures of Al powders and CNT were dried at 150 °C for 2 h in a constant-temperature bath. The dried samples were pressed at 150 kN using a cold pressing machine (Masada Seisakusho Co.,Ltd., Tokyo, Japan), which was followed by sintering at 500 °C for 2 h in a sintering furnace in air. The fabricated samples of the FGMs are illustrated in Figure 3.

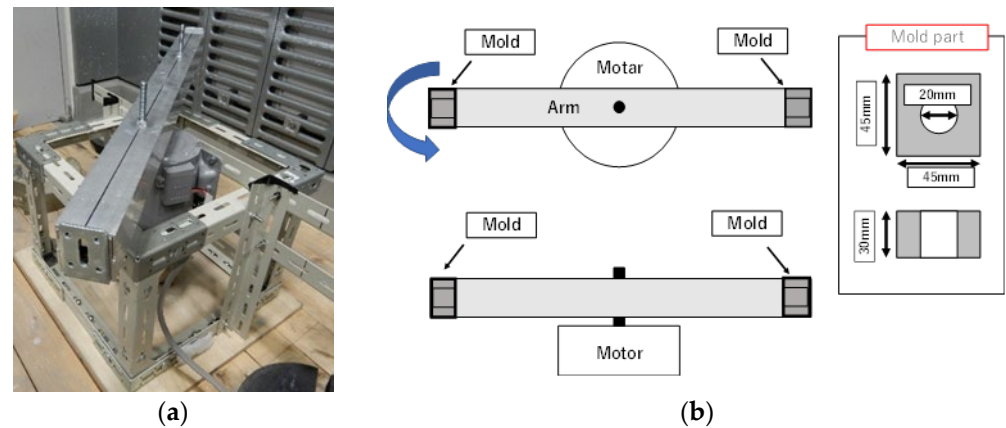


Figure 2. Set-ups of a centrifugal slurry equipment, (a) apparatus photo, and (b) schematic illustration.

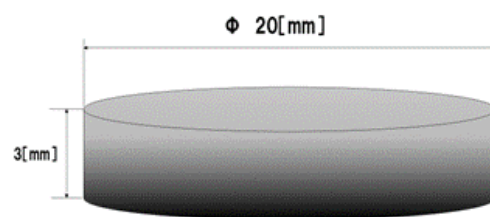


Figure 3. Schematic illustration of samples of FGMs.

2.2. Materials Characterization

Microstructure observation was conducted using a scanning electron microscope (SEM, SU8020, Hitachi High-Tech Co. Ltd., Tokyo, Japan) and energy dispersive X-ray spectrometry (EDX). Micro Vickers hardness test was conducted on the surfaces and cross sections of the test pieces of the FGMs with several points as shown in Figure 4. The load was set at 500 gW (4903 mN) and loading time was 10 s. The hardness test was conducted at 5 points in each sample. Ball-on-disk tests were conducted. Figure 5 shows an apparatus photo and schematic illustration of ball-on-disk equipment set-ups. The test conditions are tabulated in Table 1.

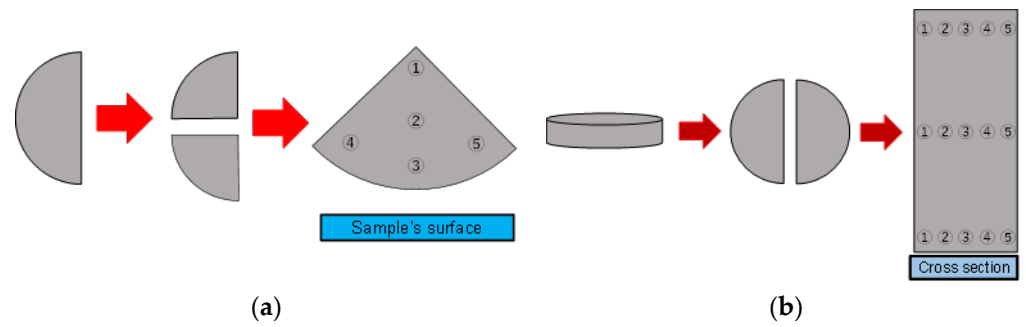


Figure 4. Micro Vickers hardness testing points on (a) surfaces, and (b) cross sections. The centrifugal force direction corresponds to ①⇒⑤ in (b).

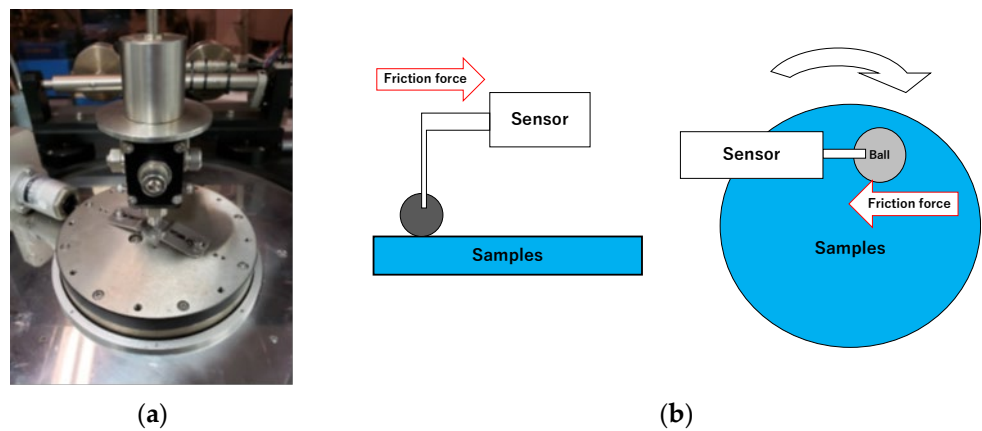


Figure 5. Ball-on-disk set-ups: (a) apparatus photo and (b) schematic illustration.

Table 1. Conditions for the ball-on-disk test.

Line Speed	Rotation Radius	Rotation Time	Direction of Rotation
10 mm/s	2 mm	1200 s	Clockwise

3. Experimental Results

3.1. Microstructures

Figure 6 shows the SEM image and EDX results for FGMs with the rotating speed of 150 rpm. Table 2 indicates the mass fraction (%) of Al and CNT in samples of FGMs fabricated with different rotation speeds. Higher rotation speeds correspond to higher centrifugal force, for which normally centrifugal force is proportional to the square of the rotation speed [11]. It is seen that, along the centrifugal force directions, segregation occurs, in which CNT moves from one side to another (from the right side to the left in Figure 6). This segregation degree depends on viscosity and density of slurry, size and density of Al powders and CNT, aspect ratio of CNT as well as rotating speeds as given by Equations (1) and (2). It is considered that centrifugal slurry methods can be effective to make a gradient of content of CNT in Al matrix, even though CNT has a cylindrical shape.

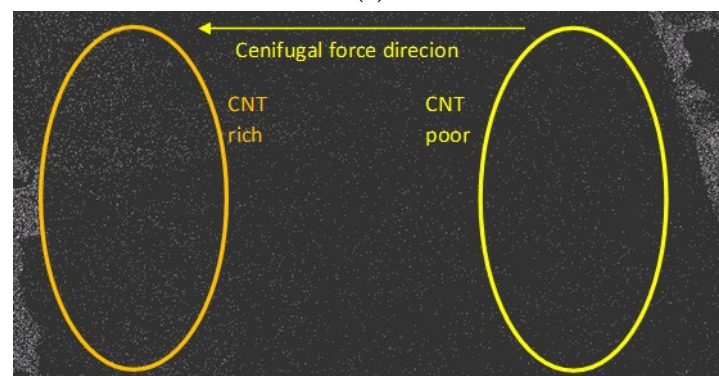
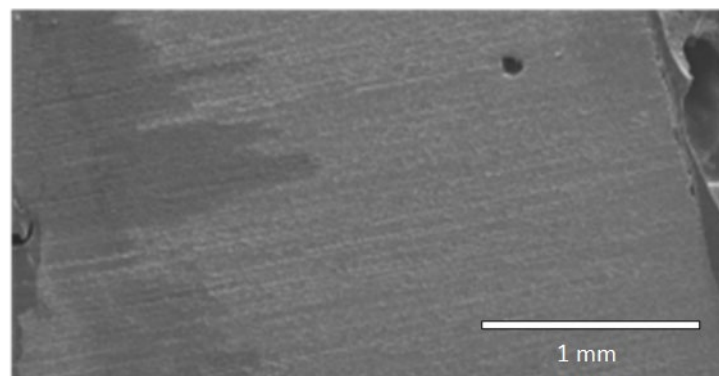


Figure 6. SEM and EDX results for FGMs with the rotating speed of 150 rpm. (a) SEM image and (b) EDX results.

Table 2. Mass fraction (%) of Al and CNT in samples of FGMs with different rotation speeds.

Rotation Speed (rpm)		CNT-Poor Side → CNT-Rich Side (Centrifugal Force Direction)			
		Spectrum ①	Spectrum ②	Spectrum ③	Spectrum ④
150	Al (mass %)	76.43	74.92	74.17	75.11
	CNT (mass %)	23.57	25.08	25.83	24.89
200	Al (mass %)	86.01	82.03	86.60	84.41
	CNT (mass %)	13.99	17.97	13.40	15.59
250	Al (mass %)	88.13	86.96	87.49	86.75
	CNT (mass %)	11.87	13.04	12.51	13.25
300	Al (mass %)	85.81	86.12	86.53	83.51
	CNT (mass %)	14.19	13.88	13.47	16.49
350	Al (mass %)	86.25	88.04	82.94	84.47
	CNT (mass %)	13.75	11.96	17.08	15.53
400	Al (mass %)	84.20	84.55	84.79	81.97
	CNT (mass %)	15.89	15.45	15.21	18.03
450	Al (mass %)	85.81	86.61	85.93	85.25
	CNT (mass %)	14.19	13.39	14.07	14.75

3.2. Mechanical Properties

Figure 7 shows Vickers hardness in the cross sections of the samples. The tendency can be seen that, for samples with any rotation speeds, as closer to the CNT-rich surface in the centrifugal force direction, hardness increases. It was confirmed that in addition to the SEM EDX data, hardness results also demonstrated the effectiveness of centrifugal slurry methods to fabricate CNT/Al matrix FGMs. Namely, in centrifugal force directions, the transfer of CNT in Al matrix can be seen from one side to another. Figure 8 shows average values of Vickers hardness of CNT-rich and CNT-poor surfaces. It is seen that except for the sample with 450 rpm, the CNT-rich surface shows higher hardness than CNT-poor one.

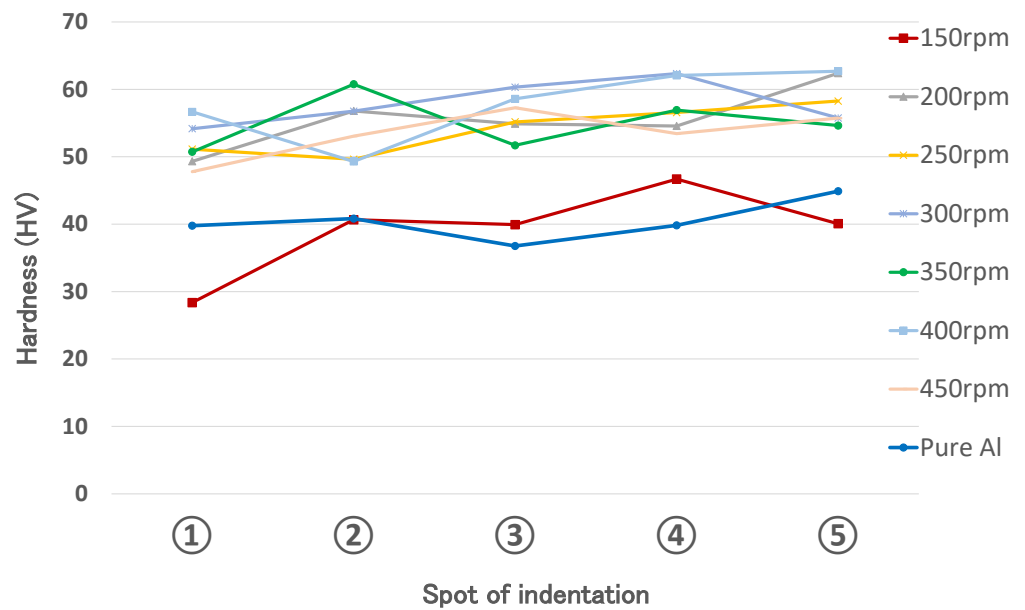


Figure 7. Vickers hardness on the cross sections for samples of FGMs with different rotation speeds. Centrifugal directions correspond to ①⇒⑤.

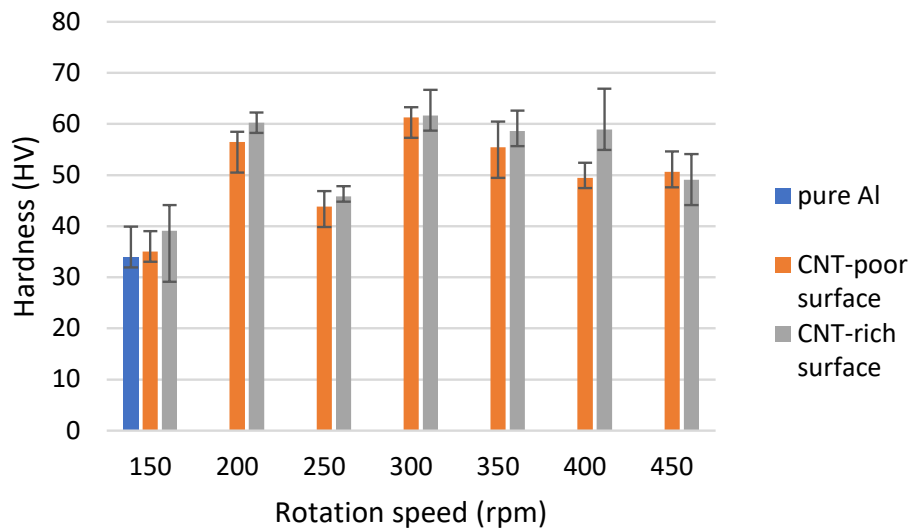


Figure 8. Vickers hardness on the CNT-rich and CNT-poor surfaces for samples with various rotation speeds. As a reference, data for pure Al is also shown.

Next, we look at tribological characteristics of the CNT/Al FGMs. Figure 9 indicates ball-on-disk test results for surfaces of pure Al, and CNT-rich surfaces of FGMs with the rotation speed of 150 rpm. It is seen that the friction force for surfaces of pure Al is almost

constant with time, while that for CNT-rich surfaces of the FGMs are waved in relatively large periods. It is considered that CNT can show high resistance to a ball movement corresponding to increase of friction force, that is, having the high coefficient of friction. Figure 10 shows probability density of friction force, including the results of samples of pure Al and FGMs with the rotation speeds from 150 to 450 rpm. This is derived from average values and standard deviations of the frictional forces. It is seen that higher friction force can be detected on CNT-rich surfaces than CNT-poor surfaces. Wider spreading in probability density of frictions, that corresponds to higher standard deviations, can be seen on the CNT-poor surfaces than CNT-rich surfaces. It is concluded that presence of CNT can lead to increase of the coefficient of friction.

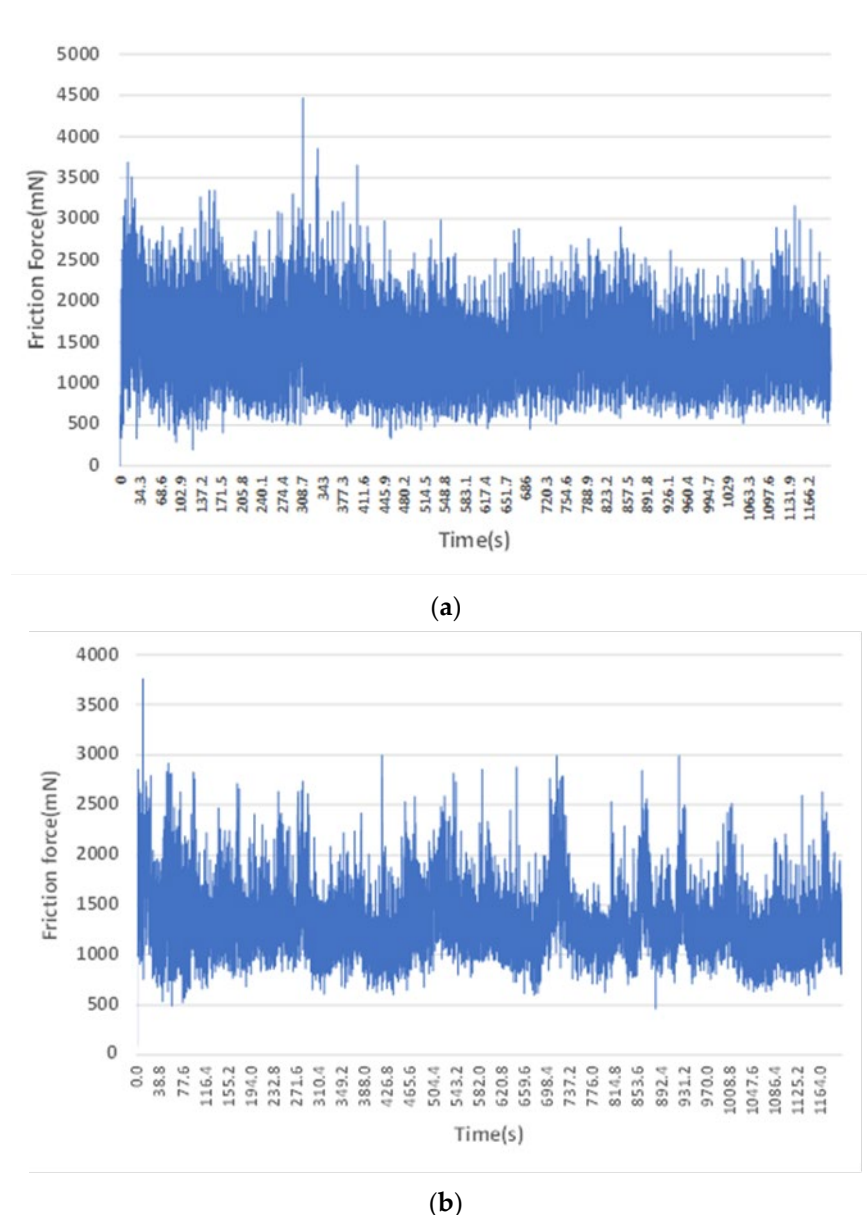


Figure 9. Ball-on-disk test results for surfaces of (a) pure Al and (b) CNT-rich surfaces of FGMs with the rotation speed of 150 rpm.

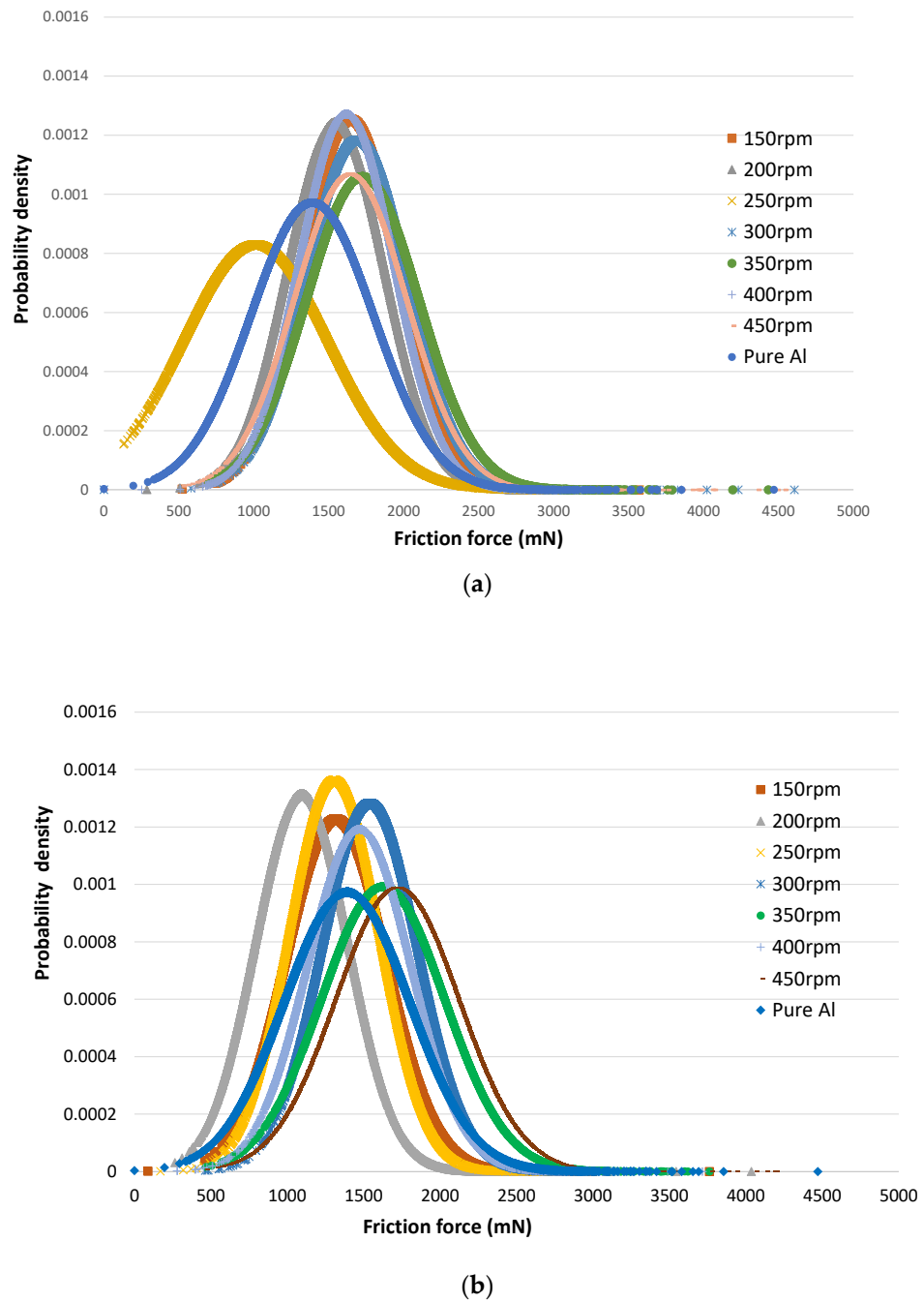


Figure 10. Probability density against friction force on (a) CNT-rich surface and (b) CNT-poor Scheme 150. to 450 rpm. (As a reference, pure Al data are also shown.).

Figure 11 shows mass reduction of samples of the FGMs with the rotation speeds from 150 to 450 rpm. It is seen that, in FGMs with the rotation speeds of 150, 250, 300 and 400 rpm, CNT-rich sides show lower mass reduction than CNT-poor sides, which may come from the idea that in CNT-rich sides, CNT was scraped off the surface before scraping of Al, leading to low mass reduction of the samples. It can be confirmed that the CNT gradient in CNT/Al matrix FGMs contributes to the enhanced wear resistance of the materials, even though the coefficient of friction increases with increasing CNT content.

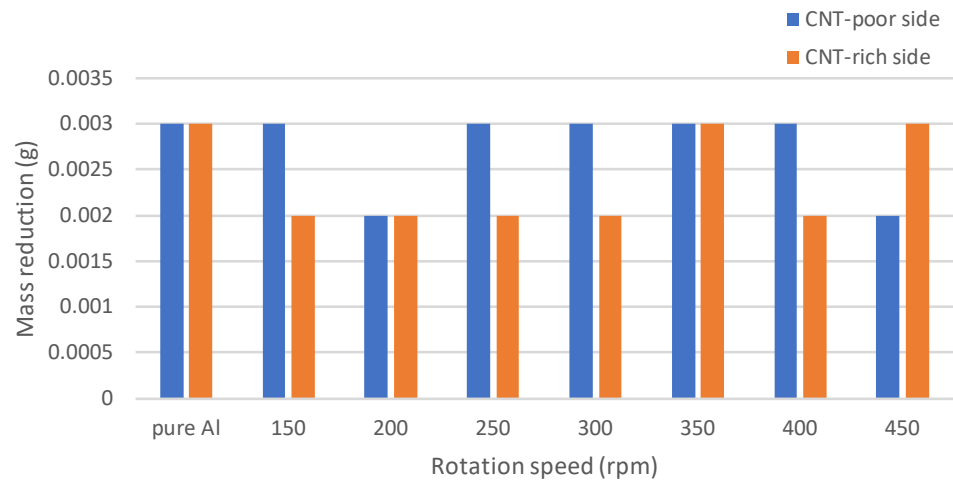


Figure 11. Mass reduction of samples of FGMs with the rotation speeds from 150 to 450 rpm.

4. Calculation of Sedimentation Velocity

It has been reported by some researchers that FGMs with particles can be fabricated by centrifugal techniques [25–28]. For such FGMs with particles, theoretical work was also reported [26]. It was demonstrated in the work [26] that the motion of particles in viscous liquid under a centrifugal force obeys the Stokes’ law. The sedimentation velocity of particles in viscous liquid under a centrifugal force can be expressed by the Stokes’ sedimentation velocity equation shown in Equation (1). The relative centrifugal acceleration G in Equation (1) can be expressed by Equation (2) [26].

$$V = \frac{Gg(\rho_s - \rho)d^2}{18\mu} \tag{1}$$

$$G = \frac{2\pi^2DN^2}{g} \tag{2}$$

Here, ρ_s is the density of the particles, ρ is the density of the fluid, d is the particle diameter, and μ is the viscosity of the fluid, $D/2$ is the radius of rotation, and N is the number of rotations. From Equations (1) and (2), the velocity of particles is proportional to the difference in density between slurry and particles, the square of the diameter of the particles, and the square of the number of revolutions, and is inversely proportional to the viscosity of the fluid.

Table 3 shows densities and particle sizes of Al and CNT, and Table 4 shows densities and viscosities of solvent (DMAs) and dispersant (K_2CO_3). Using these, sedimentation velocities of CNT and Al powders were calculated based on Stokes’ sedimentation velocity equation shown in Equation (1) dealing with the particles (shape of sphere) in the fluid, even though CNT has a cylindrical shape (tube), and CNT agglomerates in a state where tubes are entangled with each other due to strong π - π interaction and van der Waals force. In the current calculations, CNT is assumed to have a shape of sphere with diameters of the same values as the diameter (8 nm) or the length (6 μ m) of the CNT. The state of aggregation of CNT was also considered, which has the shape of sphere with a diameter of 30 μ m. In addition, it can be considered that dispersant of K_2CO_3 may surround the CNT to form sphere particles with a diameter of 50 μ m. Figure 12 shows the calculation results based on Equations (1) and (2) considering such states of CNT.

Table 3. Density and particle size of Al and CNT.

	Density (kg/m ³)	Particle Size (µm)
Al	2750	30
CNT	1000	0.008 (d), 6 (l), 30 (agg.), 50 (surrounded by K ₂ CO ₃)

Table 4. Density and viscosity of solvent (DMAs) and dispersant (K₂CO₃).

	Density (kg/m ³)	Viscosity (mPa s)
DMAs	937	0.92
K ₂ CO ₃	2300	-

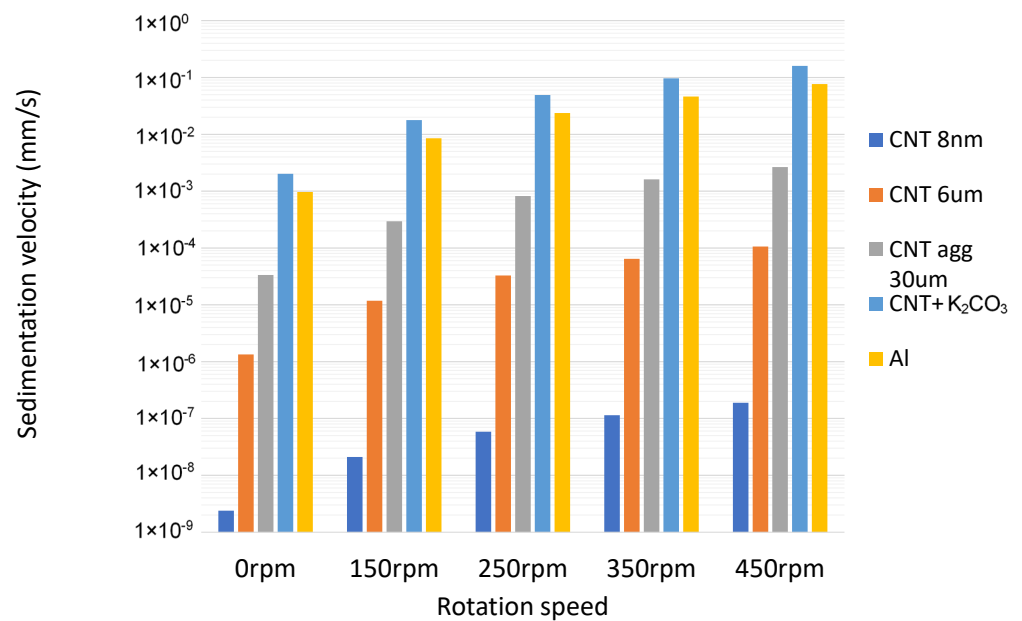


Figure 12. Sedimentation velocity of Al powders and CNT with variety of rotation speeds from 150 to 450 rpm.

It is seen in Figure 12 that sedimentation velocities of CNT of spherical shape with a diameter of 8 nm, 6 µm and 30 µm (aggregation) are lower than that of Al powders. Only CNT surrounded by K₂CO₃ (50 µm) shows higher velocity than Al powders. It is considered that there may be other factors, which cannot be expressed by Stokes’ law, to understand the motion of CNT to centrifugal directions is quicker than that of Al powders. Even so this result can provide some way to design such kinds of FGMs using centrifugal slurry methods.

5. Discussion

In the current study, CNT/Al matrix FGMs were fabricated using centrifugal slurry methods. As chemical treatments, the processes of dispersion of CNT were carried out with the solvent of DMAs, and the dispersing agent of K₂CO₃ under ultrasonic sonication conditions. As seen in Figure 6, CNT moves to the centrifugal force directions. According to the simulation results of sedimentation velocities of particles derived from Stokes’ law expressed by Equations (1) and (2), sedimentation velocity of CNT may be lower than that of Al powders as shown in Figure 12 if the shape of CNT is assumed to be spherical. However, considering the effect of dispersant of K₂CO₃ surrounding the CNT or the fibre shape of CNT not being spherical, it may be possible for CNT to move more quickly than Al powders into the centrifugal direction.

The samples of CNT/Al matrix FGMs fabricated by centrifugal slurry methods were investigated on their tribological characteristics. Such CNT/Al matrix FGMs are expected to be applied to pistons of engines in automobiles and others. Therefore, it is important to know friction force (coefficient) and the amount of reduction of the surface materials during the friction processes. It was found that the presence of CNT can contribute to high friction force, that is, high coefficient of friction. CNT-rich surfaces show higher friction force than CNT-poor surfaces. CNT-rich sides show lower mass reduction than CNT-poor sides as shown in Figure 11. It is considered that in CNT-rich sides, CNT was scraped off the surface before scraping of Al, leading to low mass reduction of the samples. It can be confirmed that the CNT gradient in CNT/Al matrix FGMs contributes to enhance wear resistance of the materials, even though the coefficient of friction increases with increasing CNT content. If the CNT orientation can be controlled, ex. by post-sintering rolling processing, etc., there is a possibility that the coefficient of friction may decrease on CNT-rich surfaces.

6. Conclusions

In this study, CNT/aluminum (Al) matrix functionally graded materials (FGMs) were fabricated using centrifugal slurry methods. Tribological characteristics on CNT/Al matrix FGMs were investigated using a ball-on-disk tribometer. The summary is described below.

1. Centrifugal slurry methods were effectively applied to obtain a gradient of content of CNT in CNT/Al matrix FGMs.
2. CNT was highly apart each other in the solvent of dimethylacetamide (DMAs) with the dispersant of potassium carbonate (K_2CO_3) under ultrasonic sonication conditions.
3. Owing to the centrifugal force, the content of CNT gradually varies in each Al matrix, which was verified by SEM EDX element analysis and Vickers hardness.
4. CNT-rich surface indicated higher frictional force as well as wear resistance (lower mass reduction) than CNT-poor surface in FGMs.
5. In order to understand formation of a gradient of CNT content by Stokes' law, it may be necessary to consider the effect of states of aggregation of CNT or CNT surrounded by dispersant of K_2CO_3 .

In future work, the orientation of CNT in the FGMs will be controlled by post-sintering mechanical treatments.

Funding: This research received no external funding.

Conflicts of Interest: The authors declare no conflict of interest.

References

1. Hanizam, H.; Sallehc, M.S.; Omar, M.Z.; Sulong, A.B. Optimisation of mechanical stir casting parameters for fabrication of carbon nanotubes-aluminium alloy composite through Taguchi method. *J. Mater. Res. Technol.* **2019**, *8*, 2223–2231. [\[CrossRef\]](#)
2. Yi, C.; Chen, X.; Gou, F.; Dmuchowski, C.M.; Sharma, A.; Park, C.; Ke, C. Direct Measurements of the Mechanical Strength of Carbon Nanotube-Aluminum Interfaces. *Carbon* **2017**, *125*, 93–102. [\[CrossRef\]](#)
3. Sridhar, I.; Narayanan, K.R. Processing and characterization of MWCNT reinforced aluminum matrix composites. *J. Mater. Sci.* **2009**, *44*, 1750–1756. [\[CrossRef\]](#)
4. Cavaliere, P.; Sadeghi, B.; Shabani, A. Carbon nanotube reinforced aluminum matrix composites produced by spark plasma sintering. *J. Mater. Sci.* **2017**, *52*, 8618–8629. [\[CrossRef\]](#)
5. Matsumoto, K.; Takahashi, T.; Ishii, S.; Jikei, M. Investigation of Dispersibility of Multi-Walled Carbon Nanotubes Using Polysulfones with Various Structures. *Int. J. Soc. Mater. Eng. Resour.* **2014**, *20*, 77–81. [\[CrossRef\]](#)
6. Khanna, V.; Kumar, V.; Bansal, S.A. Mechanical properties of aluminium-graphene/carbon nanotubes (CNTs) metal matrix composites: Advancement, opportunities and perspective. *Mater. Res. Bull.* **2021**, *138*, 111224. [\[CrossRef\]](#)
7. Velmurugan, V.; Reddy, L.V.K.; Thanikaikarasan, S. A study on mechanical characterization of carbon nanotube reinforced metal matrix composites. *Mater. Today Proc.* **2020**, *33*, 3520–3524. [\[CrossRef\]](#)
8. Tsukamoto, H. Enhanced Mechanical Properties of Carbon Nanotube-Reinforced Magnesium Composites with Zirconia Fabricated by Spark Plasma Sintering. *J. Comp. Mater.* **2021**, *55*, 2503–2512. [\[CrossRef\]](#)
9. Merino, C.A.I.; Sillas, J.E.L.; Meza, J.M.; Ramirez, J.M.H. Metal matrix composites reinforced with carbon nanotubes by an alternative technique. *J. Alloys Compd.* **2017**, *707*, 257–263. [\[CrossRef\]](#)

10. Aristizabal, K.; Katzensteiner, A.; Bachmaier, A.; Mücklich, F.; Suarez, S. Study of the structural defects on carbon nanotubes in metal matrix composites processed by severe plastic deformation. *Carbon* **2017**, *125*, 156–161. [[CrossRef](#)]
11. Zhou, W.; Sun, X.; Kikuchi, K.; Nomura, N.; Yoshimi, K.; Kawasaki, A. Carbon nanotubes as a unique agent to fabricate nanoceramic/metal composite powders for additive manufacturing. *Mater. Des.* **2018**, *137*, 276–285. [[CrossRef](#)]
12. Sathish, T.; Mohanavel, V.; Ansari, K.; Saravanan, R.; Karthick, A.; Afzal, A.; Alamri, S.; Saleel, C.A. Synthesis and characterization of mechanical properties and wire cut EDM process parameters analysis in AZ61 magnesium alloy+ B₄C+ SiC. *Materials* **2021**, *14*, 3689. [[CrossRef](#)]
13. Alekseev, A.V.; Yesikov, M.A.; Strekalov, V.V.; Mali, V.I.; Khasin, A.A.; Predtechensky, M.R. Effect of single wall carbon nanotubes on strength properties of aluminum composite produced by spark plasma sintering and extrusion. *Mater. Sci. Eng. A* **2020**, *793*, 139746. [[CrossRef](#)]
14. Thirugnanasambantham, K.G.; Sankaramoorthy, T.; Karthikeyan, R.; Kumar, K.S. A comprehensive review: Influence of the concentration of carbon nanotubes (CNT) on mechanical characteristics of aluminium metal matrix composites: Part 1. *Mater. Today Proc.* **2021**, *45*, 2561–2566. [[CrossRef](#)]
15. Thirugnanasambantham, K.G.; Sankaramoorthy, T.; Vaysakh, M.; Nadish, S.Y.; Madhavan, S. A critical review: Effect of the concentration of carbon nanotubes (CNT) on mechanical characteristics of aluminium metal matrix composites: Part 2. *Mater. Today Proc.* **2021**, *45*, 2890–2896. [[CrossRef](#)]
16. Chen, B.; Zhou, X.Y.; Zhang, B.; Kondoh, K.; Li, J.S.; Qian, M. Microstructure, tensile properties and deformation behaviors of aluminium metal matrix composites co-reinforced by ex-situ carbon nanotubes and in-situ alumina nanoparticles. *Mater. Sci. Eng. A* **2020**, *795*, 139930. [[CrossRef](#)]
17. Aranke, O.; Gandhi, C.; Dixit, N.; Kuppan, P. Influence of Multiwall Carbon Nanotubes (MWCNT) on Wear and Coefficient of Friction of Aluminium (Al 7075) Metal Matrix Composite. *Mater. Today Proc.* **2018**, *5*, 7748–7757. [[CrossRef](#)]
18. Tsukamoto, H. Enhanced Mechanical Properties of Carbon Nanotube/Aluminum Composites Fabricated by Powder Metallurgical and Repeated Hot-Rolling Techniques. *J. Compos. Sci.* **2020**, *4*, 169–178. [[CrossRef](#)]
19. Tsukamoto, H. Design against fracture of functionally graded thermal barrier coatings using transformation toughening. *Mater. Sci. Eng. A* **2010**, *527*, 3217–3226. [[CrossRef](#)]
20. Tsukamoto, H. Analytical method of inelastic thermal stresses in a functionally graded material plate by a combination of micro- and macro mechanical approaches. *Compos. B Eng.* **2003**, *34*, 561–568. [[CrossRef](#)]
21. Tsukamoto, H. Microstructure and indentation properties of ZrO₂/Ti functionally graded materials fabricated by spark plasma sintering. *Mater. Sci. Eng. A* **2015**, *640*, 338–349. [[CrossRef](#)]
22. Luo, Y.W.; Ma, T.; Shao, W.W.; Zhang, G.P.; Zhang, B. Effects of heat treatment on microstructures and mechanical properties of GH4169/K418 functionally graded material fabricated by laser melting deposition. *Mater. Sci. Eng. A* **2021**, *821*, 141601. [[CrossRef](#)]
23. Sam, M.; Jojith, R.; Radhika, N. Progression in manufacturing of functionally graded materials and impact of thermal treatment—A critical review. *J. Manuf. Processes* **2021**, *68*, 1339–1377. [[CrossRef](#)]
24. Saleh, B.; Jiang, J.; Fathi, R.; Al-hababi, T.; Xu, Q.; Wang, L.; Song, D.; Ma, A. 30 Years of functionally graded materials: An overview of manufacturing methods, Applications and Future Challenges. *Compos. B Eng.* **2020**, *201*, 108376. [[CrossRef](#)]
25. El-Galy, I.M.; Ahmed, M.H.; Bassiouny, B.I. Characterization of functionally graded Al-SiCp metal matrix composites manufactured by centrifugal casting. *Alex. Eng. J.* **2017**, *56*, 371–381. [[CrossRef](#)]
26. Ogawa, T.; Watanabe, Y.; Sato, H.; Kim, I.-S.; Fukui, Y. Theoretical study on fabrication of functionally graded material with density gradient by a centrifugal solid-particle method. *Compos. Part A* **2006**, *37*, 2194–2200. [[CrossRef](#)]
27. Chumanov, I.V.; Anikeev, A.N.; Chumanov, V.I. Fabrication of functionally graded materials by introducing wolframium carbide dispersed particles during centrifugal casting and examination of FGM's structure. *Procedia Eng.* **2015**, *129*, 816–820. [[CrossRef](#)]
28. Rajan, T.P.D.; Pillai, R.M.; Pai, B.C. Characterization of centrifugal cast functionally graded aluminum-silicon carbide metal matrix composites. *Mater. Charact.* **2010**, *61*, 923–928. [[CrossRef](#)]